

$\delta(\omega - \omega')$. Any nontrivial phase ($0 < \phi < 2\pi$) in Eq. (1d) enables quantum computation, but we are interested in the case $\phi = \pi$, which corresponds to the CPHASE gate.

To characterize the action of a medium on multimode light, we use the S-matrix from scattering theory. The S-matrix is a unitary matrix connecting asymptotic input and output field states i.e. $|\omega_{\text{out}}\rangle = S|\nu_{\text{in}}\rangle$, while capturing the relevant effects of the medium. The *ideal* S-matrices corresponding to Eqs. (1a) to (1d) would be $S_{\text{id},1}(\omega_k; \nu_k) = \delta(\omega_k - \nu_k)$, for single-photon states, and $S_{\text{id},2}(\omega_a, \omega_b; \nu_a, \nu_b) = e^{i\phi} S_{\text{id},1}(\omega_a; \nu_a) S_{\text{id},1}(\omega_b; \nu_b)$ for two-photon states, where input (output) frequencies are denoted by ν_k (ω_k), for $k = \{a, b\}$. Typically, however, the *actual* S-matrices for matter-mediated interactions are of the form $S_{\text{act},1}(\omega_k; \nu_k) = e^{i\phi_k} \delta(\omega_k - \nu_k)$ and $S_{\text{act},2}(\omega_a, \omega_b; \nu_a, \nu_b) = S_{\text{act},1}(\omega_a; \nu_a) S_{\text{act},1}(\omega_b; \nu_b) + C\delta(\omega_a + \omega_b - \nu_a - \nu_b)$, where the coefficient C depends on all frequencies and the parameters of the interaction mediators [27, 28]. The phase $e^{i\phi_k}$ in $S_{\text{act},1}$ leads to a deformation of the single-photon wave packets, while the function $\delta(\omega_a + \omega_b - \nu_a - \nu_b)$ in $S_{\text{act},2}$, which arises from energy conservation [27], is usually identified as the source of spectral entanglement.

One important choice we make is to ignore single-photon deformation, which is enforced by mapping all S-matrices as $S \rightarrow S_{\text{act},1}^\dagger(\omega_a; \nu_a) S_{\text{act},1}^\dagger(\omega_b; \nu_b) S$. Most previous proposals do not do this (e.g. [15]), which accounts for part of the discrepancy in the maximum fidelities obtained. Single-photon deformation could have two negative effects for our proposal. First, it might disrupt linear-optical steps of the computation. This can be avoided by ensuring all photons are deformed equally at each computational time step [29]. Second, our results are obtained for specific input wave packet shapes, so single-photon effects could significantly degrade the fidelity of subsequent gates; later, we show that this is not the case for a few rounds of deformation. It is then possible to use measurement-based quantum computing, where each photon experiences at most two CPHASE gates [30], or teleportation-based error correction [31]. Finally, it is also possible to physically undo this deformation if necessary, as proposed e.g. in Ref. [19].

Ideally, we would like to show that the S-matrix for our proposal approaches $S_{\text{id},2}$ in some limit. However, it is sufficient for this to hold only for the particular states that we are considering. Thus, to gauge the quality of our operation, we use the average gate fidelity [32]

$$F(\phi) := \int d\psi \langle \psi | S_{\text{id}}(\phi)^\dagger S_{\text{act}} |\psi\rangle \langle \psi | S_{\text{act}}^\dagger S_{\text{id}}(\phi) |\psi\rangle \quad (2)$$

where the integration is taken over the Haar measure of the joint Hilbert space (for further details, see Appendix A). For our gate to be useful for quantum computation, it suffices that $F = 1 - \epsilon$, where ϵ is some constant threshold [33].

Single- and two-site gate fidelities. We begin by examining F for wave packets scattering from a single site, as well as two sites in a co- and counter-propagating ar-

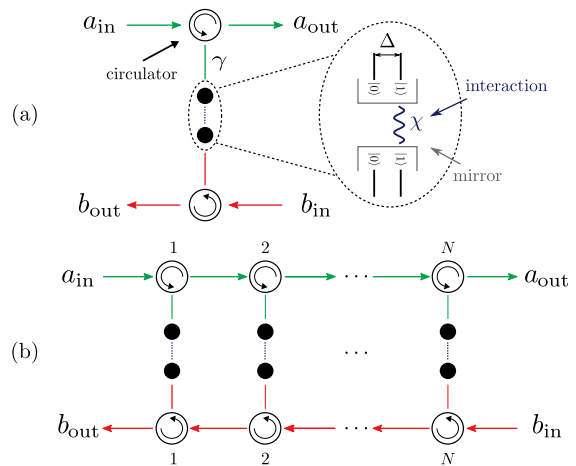


FIG. 1. (Color Online) (a) The physical system inside our unit cell. It consists of two coupled two-level atoms, with internal energies Δ , and which interact via $H = \chi(\mathbb{1} - A_z)(\mathbb{1} - B_z) = \chi|1, 1\rangle\langle 1, 1|$. The input-output fields couple to the atoms via the relation $a_{\text{out}} = \sqrt{\gamma}A_- + a_{\text{in}}$, and similarly for mode b . It was shown in Ref. [28] that this system gives rise to the same S-matrices for single- and two-photon scattering as a pair of crossed cavities with cross-Kerr interaction between them. In the limit $\chi \rightarrow \infty$, this reduces to a three-level atom in a “V” configuration, such as considered in Ref. [19]. (b) Our main proposal using N discrete interaction sites with counter-propagating photons.

range. The discrete Kerr interaction we consider is depicted in Fig. 1 (a). The unit cell we repeat in Fig. 1 (b), call it $G = (L, H)$, can be described using “LH” [34–36] parameters from input-output theory, where L is a vector of operators that couple the field to the system and H is the system Hamiltonian. The LH parameters for our unit cell are

$$G = \left[\begin{pmatrix} \sqrt{\gamma}A_- \\ \sqrt{\gamma}B_- \end{pmatrix}, \frac{\Delta}{2}(\mathbb{1} - A_z) + \frac{\Delta}{2}(\mathbb{1} - B_z) + \chi(\mathbb{1} - A_z)(\mathbb{1} - B_z) \right], \quad (3)$$

where A_- and A_z are the atomic lowering and Pauli Z operators for atom A , and likewise for B_- and B_z . We cascaded N unit cells with co- and counter-propagating fields and computed the corresponding S-matrices, as detailed in Ref. [28] and which we reproduce in Appendix B. The final ingredient needed to calculate F is the wave packet shape, which we choose to be Gaussian with detuning ω_0 (i.e. carrier frequency $\omega_c = \Delta + \omega_0$) and bandwidth σ , i.e.

$$\xi(\omega) = \frac{1}{(2\pi\sigma^2)^{1/4}} \exp \left[-\frac{(\omega - \omega_c)^2}{4\sigma^2} \right]. \quad (4)$$

In Fig. 2, column 1, we display the plots for parameters (ω_0, γ, χ) which maximize the fidelity of counter-propagating wave packets. Relative to the single site, we observe a clear increase of the maximum obtainable fidelity when the photons are counter-propagating, and a

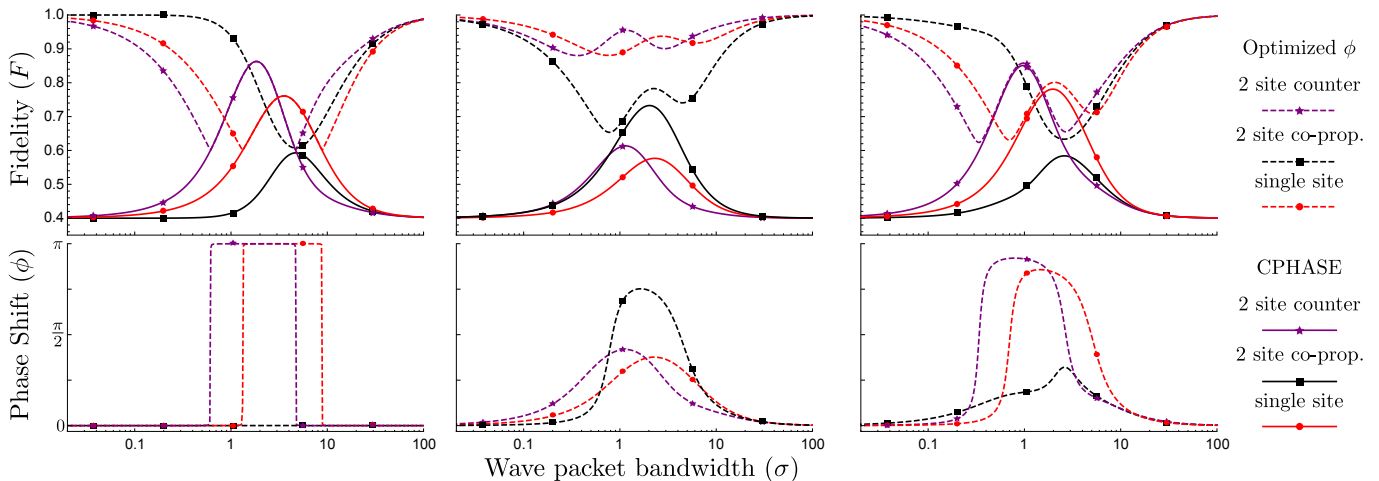


FIG. 2. (Color online). In the top row, solid lines represent the average gate fidelity with respect to the CPHASE gate, i.e. $F(\phi = \pi)$, while dashed lines denote the fidelity $F(\phi)$ maximized with respect to some ϕ . The second row plots the corresponding phase shift $\phi_{\text{opt}} = \text{argmax}_{\phi} F(\phi)$. We compare three cases of interest: (i) a single-site Kerr interaction (circles), (ii) a two-site interaction with co-propagating photons (squares), (iii) the two-site interaction with counter-propagation (stars). In column 1, we have chosen $(\omega_0, \gamma, \chi) = (0, 10, 10000)$, which maximizes F for the counter-propagating case, resulting in $F_{\text{counter}} = 0.8628$ (only for this case, whenever $F \gtrsim 0.6$, the dashed and solid lines coincide). In column 2 we chose $(\omega_0, \gamma, \chi) = (0, 6, 2.67)$ to maximize F for the co-propagating case obtaining $F_{\text{co-prop.}} = 0.7326$, and in column 3 we chose $(\omega_0, \gamma, \chi) = (1.1, 4.5, 5)$ to optimize the single-site F , obtaining $F_{\text{single}} = 0.7810$.

decrease when they are co-propagating, as illustrated in the top row. In the limit of large χ and $\omega_0 = 0$, the phase shift is always either 0 or π , corresponding to the identity or CPHASE gate respectively (see the second row). We observe that counter-propagating wave packets tend to perform better than co-propagating for a large region of the parameter space, but there are exceptions.

In Fig. 2, column 2, we display a parameter regime where co-propagating photons obtain their maximum fidelity and outperform the other two cases. The explanation for this is the following. In this regime, the co-propagating case seems to suffer more spectral entanglement, but also acquire a larger phase shift, than the other two (see the dashed lines), and the tradeoff between these effects leads to a higher fidelity with the CPHASE gate. However, these effects are linked in such a way that this peak fidelity and the maximum phase are still much inferior to the best obtained by the single-site and counter-propagating cases in other parameter regimes. Nonetheless, this suggests it is possible to use a perturbative approach to construct long weakly-coupled atom chains where the rate at which phases and spectral entanglement accumulate are more benign (e.g. [19]). It is also interesting that the peak of the fidelity in the co-propagating case happens for larger σ than for the counter-propagating case in all three columns, which could lead to a CPHASE gate for spectrally broader photons.

In Fig. 2, column 3, we display parameters that maximize the single-site fidelity. As we generically expect, the counter-propagating wave packets outperform the single-site and co-propagating ones both in fidelities and phase shifts. This happens even when $\omega_0 \neq 0$, indicating that

our conclusions are somewhat robust with respect to being off-resonance.

N-site gate fidelities. We now investigate the average fidelity of our proposal to the CPHASE gate as we increase the number of interaction sites. Based on observations from the two-site case, we restrict our analysis to counter-propagating photons, working on-resonance ($\omega_0 = 0$), and take a $\chi \rightarrow \infty$ limit, since this yields the most promising results. We also take $\gamma = 1$, since choosing other values effectively rescales σ when working on-resonance. Thus, the average gate fidelity F is a function of the number of interaction sites N and the photon bandwidth σ : $F(\sigma, N)$.

In Fig. 3(a) we plot the average gate fidelity, as a function of σ , for increasing N . Notice that, as the number of interaction sites increases, the maximum average fidelity increases, indicating that the resulting operation is sequentially closer to a CPHASE gate. Also notice that, besides attaining higher maximum values, the fidelity curve is also becoming broader (albeit in logarithmic scale). This means that, as the number of sites is increased, the proposed CPHASE gate becomes more broadband, or robust with respect to the spectral bandwidth of the photon. The highest value for the fidelity in Fig. 3(a) is 0.996, when $N = 20$.

In Fig. 3(b), we investigate the maximum of the average fidelity F_{max} and its corresponding value of σ_{max} as a function of N . We see that $1 - F_{\text{max}}$ is monotonically decreasing and σ_{max} slowly tends towards the plane-wave limit. For the observed behaviour of Fig. 3(a-b) we predict that, in order to obtain $F_{\text{max}} = 0.999$, we would need $N \simeq 50$ and $\sigma \simeq 0.014\text{s}^{-1}$. Fig. 3(b) also shows that, for

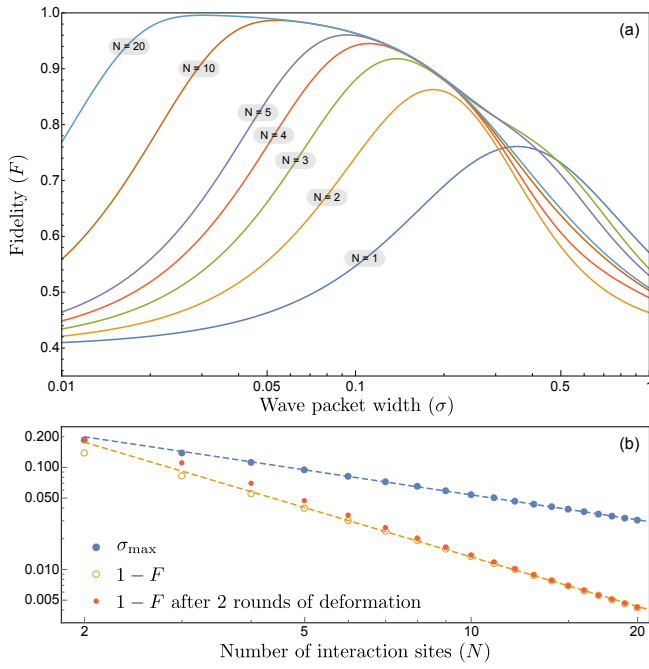


FIG. 3. (Color online). (a) Average gate fidelity between our proposal and the CPHASE as a function of frequency bandwidth σ for increasing number of interaction sites N . (b) We take the maximum of the gate fidelity in (a), and plot the infidelity $(1 - F)$ and the corresponding maximizing σ_{\max} as functions of the number of interaction sites N . Small red dots correspond to $1 - F$ for photons that have undergone two rounds of single-photon deformation. The dashed lines correspond to the fits $1 - F(\sigma_{\max}, N) = 0.537N^{-1.61}$ and $\sigma_{\max} = 0.350N^{-0.81}$, where we fit to $N \in [4, 20]$.

$N > 5$, the fidelity is not significantly affected by using single-photon wave packets that have suffered one or two rounds of deformation.

Another feature apparent in Fig. 3(a) is that, for fixed σ , the advantage gained from increasing N eventually saturates. This is explored further in Fig. 4. An intuitive explanation is: interpret $1/\gamma$ as the typical timescale before an excited atom re-emits a photon, then $t_m \approx N/\gamma$ is the time that each wave packet remains inside the medium. Thus, if the wave packets have temporal width of $t_w \approx 1/\sigma$, when N is roughly γ/σ the chain becomes “long enough” to contain the entire wave packets, and the interaction saturates.

Our results show that, to obtain higher-fidelity gates, one has to move to smaller values of σ together with longer atomic chains. In fact, in Ref. [28], we and Gea-Banacloche have shown that, in the limit where $\sigma \rightarrow 0$ and $N \rightarrow \infty$, the S-matrix for the N -site case tends to the ideal one (modulo single-photon deformation) $S_2(\omega_a, \omega_b; \nu_a, \nu_b) = -S_{\text{act},1}(\omega_a; \nu_a)S_{\text{act},1}(\omega_b; \nu_b)$. This is independent of the specific wave packet shape, further motivating our choice to ignore single-photon deformation. The results presented here are more relevant for implementations, as one only needs to increase N and

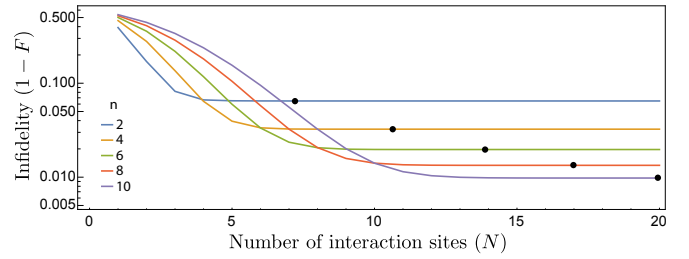


FIG. 4. (Color online). Saturation of the average gate infidelity for fixed σ as the number of interaction sites N increases. For illustration, we choose the σ 's that maximize the fidelity for specific numbers of interaction sites n , i.e. $\sigma_{\max}^n = \text{argmax}_{\sigma} F(\sigma, n)$ where $n = \{2, 4, 6, 8, 10\}$. The lines then correspond to the fidelities at σ_{\max}^n for increasing N , i.e. $F(\sigma_{\max}^n, N)$. Finally, the black dots in each curve correspond to $N = 1/\sigma_{\max}^n$, where we predict the fidelity to saturate.

decrease σ until the fidelity surpasses the threshold necessary for fault-tolerant computation.

Discussion. Our goal was to determine if it possible to build a passive CPHASE gate using cross-Kerr interactions, and we have shown that it is. Importantly, our results do not contradict those of Ref. [14], which uses a phenomenological model of a cross-Kerr medium. Using that model, a CPHASE gate might indeed be unachievable. However, our results are based on a fully multimode treatment of the field and a fully microscopic treatment of the interaction mediators. Thus we believe they do provide a counter-example against the stronger claim, which is frequently propagated in the literature, that the multimode nature of the field is a fundamental physical obstacle to implementing a CPHASE gate. Furthermore, our proposal enjoys two advantages over prior proposals. First, our gate is passive, i.e., it does not require active error correction, such as the principal mode projection technique used in Ref. [19]. Also, our proposal requires fewer interaction sites to achieve a fixed fidelity, e.g. in Ref. [19] the authors estimate they need 10^6 interaction sites for a 95% fidelity with a CPHASE gate, whereas our proposal achieves that value with 5 sites.

Admittedly, our proposal is a proof-of-principle result that will be challenging to construct in practice. Further, we hope our construction will inspire others to devise simpler and less resource-intensive proposals. There are plenty of avenues to explore, e.g. placing the atomic interaction sites inside cavities to gain a cavity enhancement [37], or varying the atom parameters along the chain [38] while simultaneously varying the input photon wave packet shape. Our analysis did not include any additional imperfections, and we leave as future work to adapt our model to include other effects such as losses, emission into non-guided modes, coupling to a thermal bath, etc. In Appendix C we propose an update to a set of rules, initially laid out by Gea-Banacloche [15], that must be satisfied by any theoretical proposal for a realistic CPHASE gate, based on conclusions drawn from this work and [28].

The authors acknowledge helpful discussions with Agata Brańczyk, Daniel Gottesman, Bing He, Raissa Mendes, Barry Sanders, and Zak Webb. The authors also thank Julio Gea-Banacloche and Jeffrey Shapiro for feedback and friendly discussions about this work. This

research was supported by Perimeter Institute for Theoretical Physics. Research at Perimeter Institute is supported by the Government of Canada through the Department of Innovation, Science and Economic Development Canada and by the Province of Ontario through the Ministry of Research, Innovation and Science.

-
- [1] R. Karplus and M. Neuman, “Non-linear interactions between electromagnetic fields,” *Phys. Rev.* **80**, 380 (1950).
- [2] P. Kok, W. J. Munro, K. Nemoto, T. C. Ralph, J. P. Dowling, and G. J. Milburn, “Linear optical quantum computing with photonic qubits,” *Rev. Mod. Phys.* **79**, 135 (2007).
- [3] M. A. Nielsen and I. L. Chuang, *Quantum computation and quantum information* (Cambridge university press, 2010).
- [4] E. Knill, R. Laflamme, and G. J. Milburn, “A scheme for efficient quantum computation with linear optics,” *Nature* **409**, 46 (2001).
- [5] M. A. Nielsen, “Optical quantum computation using cluster states,” *Phys. Rev. Lett.* **93**, 040503 (2004).
- [6] N. C. Menicucci, “Fault-tolerant measurement-based quantum computing with continuous-variable cluster states,” *Phys. Rev. Lett.* **112**, 120504 (2014).
- [7] M. Gimeno-Segovia, P. Shadbolt, D. E. Browne, and T. Rudolph, “From three-photon Greenberger-Horne-Zeilinger states to ballistic universal quantum computation,” *Phys. Rev. Lett.* **115**, 020502 (2015).
- [8] G. J. Milburn, “Quantum optical Fredkin gate,” *Phys. Rev. Lett.* **62**, 2124 (1989).
- [9] I. L. Chuang and Y. Yamamoto, “Simple quantum computer,” *Phys. Rev. A* **52**, 3489 (1995).
- [10] V. Venkataraman, K. Saha, and A. L. Gaeta, “Phase modulation at the few-photon level for weak-nonlinearity-based quantum computing,” *Nat Photon* **7**, 138 (2013).
- [11] Q. A. Turchette, C. J. Hood, W. Lange, H. Mabuchi, and H. J. Kimble, “Measurement of conditional phase shifts for quantum logic,” *Phys. Rev. Lett.* **75**, 4710 (1995).
- [12] I.-C. Hoi, A. F. Kockum, T. Palomaki, T. M. Stace, B. Fan, L. Tornberg, S. R. Sathyamoorthy, G. Johansson, P. Delsing, and C. M. Wilson, “Giant cross-Kerr effect for propagating microwaves induced by an artificial atom,” *Phys. Rev. Lett.* **111**, 053601 (2013).
- [13] K. M. Beck, M. Hosseini, Y. Duan, and V. Vuletić, “Large conditional single-photon cross-phase modulation,” [arXiv:1512.02166](https://arxiv.org/abs/1512.02166) (2015).
- [14] J. H. Shapiro, “Single-photon Kerr nonlinearities do not help quantum computation,” *Phys. Rev. A* **73**, 062305 (2006).
- [15] J. Gea-Banacloche, “Impossibility of large phase shifts via the giant Kerr effect with single-photon wave packets,” *Phys. Rev. A* **81**, 043823 (2010).
- [16] L. Boivin, F. X. Kärtner, and H. A. Haus, “Analytical solution to the quantum field theory of self-phase modulation with a finite response time,” *Phys. Rev. Lett.* **73**, 240 (1994).
- [17] L.-M. Duan and H. J. Kimble, “Scalable photonic quantum computation through cavity-assisted interactions,” *Phys. Rev. Lett.* **92**, 127902 (2004).
- [18] K. Koshino, S. Ishizaka, and Y. Nakamura, “Deterministic photon-photon $\sqrt{\text{swap}}$ gate using a Λ system,” *Phys. Rev. A* **82**, 010301 (2010).
- [19] C. Chudzicki, I. L. Chuang, and J. H. Shapiro, “Deterministic and cascaded conditional phase gate for photonic qubits,” *Phys. Rev. A* **87**, 042325 (2013).
- [20] T. C. Ralph, I. Söllner, S. Mahmoodian, A. G. White, and P. Lodahl, “Photon sorting, efficient bell measurements, and a deterministic controlled- z gate using a passive two-level nonlinearity,” *Phys. Rev. Lett.* **114**, 173603 (2015).
- [21] B. Hacker, S. Welte, G. Rempe, and S. Ritter, “A photon-photon quantum gate based on a single atom in an optical resonator,” *Nature advance online publication*, (2016).
- [22] A. M. Childs, D. Gosset, and Z. Webb, “Universal computation by multiparticle quantum walk,” *Science* **339**, 791 (2013).
- [23] M. Mašalas and M. Fleischhauer, “Scattering of dark-state polaritons in optical lattices and quantum phase gate for photons,” *Phys. Rev. A* **69**, 061801 (2004).
- [24] I. Friedler, D. Petrosyan, M. Fleischhauer, and G. Kurizki, “Long-range interactions and entanglement of slow single-photon pulses,” *Phys. Rev. A* **72**, 043803 (2005).
- [25] A. V. Gorshkov, J. Otterbach, M. Fleischhauer, T. Pohl, and M. D. Lukin, “Photon-photon interactions via Rydberg blockade,” *Phys. Rev. Lett.* **107**, 133602 (2011).
- [26] A. V. Gorshkov, J. Otterbach, E. Demler, M. Fleischhauer, and M. D. Lukin, “Photonic phase gate via an exchange of fermionic spin waves in a spin chain,” *Phys. Rev. Lett.* **105**, 060502 (2010).
- [27] S. Xu, E. Rephaeli, and S. Fan, “Analytic properties of two-photon scattering matrix in integrated quantum systems determined by the cluster decomposition principle,” *Phys. Rev. Lett.* **111**, 223602 (2013).
- [28] D. J. Brod, J. Combes, and J. Gea-Banacloche, “Two photons co- and counter-propagating through N cross-Kerr sites,” *Phys. Rev. A* **94**, 023833 (2016).
- [29] This can be done e.g. by passing photons through empty cavities or uncoupled atoms.
- [30] A. M. Childs, D. W. Leung, and M. A. Nielsen, “Unified derivations of measurement-based schemes for quantum computation,” *Phys. Rev. A* **71**, 032318 (2005).
- [31] Specifically, photonic qubits which have experienced M rounds of CPHASE gates can be teleported onto wave packets which have only experienced one round of distortion.
- [32] M. A. Nielsen, “A simple formula for the average gate fidelity of a quantum dynamical operation,” *Physics Letters A* **303**, 249 (2002).
- [33] Y. R. Sanders, J. J. Wallman, and B. C. Sanders, “Bounding quantum gate error rate based on reported average fidelity,” *New Journal of Physics* **18**, 012002 (2016).

- [34] H. J. Carmichael, “Quantum trajectory theory for cascaded open systems,” *Phys. Rev. Lett.* **70**, 2273 (1993).
- [35] C. W. Gardiner, “Driving a quantum system with the output field from another driven quantum system,” *Phys. Rev. Lett.* **70**, 2269 (1993).
- [36] J. Gough and M. James, “The series product and its application to quantum feedforward and feedback networks,” *Automatic Control, IEEE Transactions on* **54**, 2530 (2009).
- [37] B. Fan, G. Johansson, J. Combes, G. J. Milburn, and T. M. Stace, “Nonabsorbing high-efficiency counter for itinerant microwave photons,” *Phys. Rev. B* **90**, 035132 (2014).
- [38] M. R. Hush, A. R. R. Carvalho, M. Hedges, and M. R. James, “Analysis of the operation of gradient echo memories using a quantum input-output model,” *New Journal of Physics* **15**, 085020 (2013).
- [39] V. Kendon, K. Nemoto, and W. Munro, “Typical entanglement in multiple-qubit systems,” *Journal of Modern Optics* **49**, 1709 (2002).

Appendix A: Average gate fidelity

In this paper, we gauge the quality of our operation using the standard average gate fidelity [32]:

$$F_1(\phi) := \int d\psi \langle \psi | S_{\text{id}}(\phi)^\dagger S_{\text{act}} | \psi \rangle \langle \psi | S_{\text{act}}^\dagger S_{\text{id}}(\phi) | \psi \rangle \quad (\text{A1})$$

where the integration is over the two-qubit Haar measure, and S_{id} and S_{act} include the removal of the single-photon deformation. Equation (A1) is the same as Eq. (2) in the main text. In order to carry out the averaging explicitly, one parameterizes $|\psi\rangle$ as [39]

$$|\psi\rangle = e^{i\chi_0} \cos \theta_0 |00\rangle + e^{i\chi_1} \sin \theta_0 \cos \theta_1 |01\rangle + e^{i\chi_2} \sin \theta_0 \sin \theta_1 \cos \theta_2 |10\rangle + e^{i\chi_3} \sin \theta_0 \sin \theta_1 \sin \theta_2 |11\rangle,$$

where $0 \leq \chi_i < 2\pi$ and $0 \leq \theta_i < \pi/2$. In this parameterization, the Haar measure in the integration is

$$d\psi = 48(2\pi)^{-4} (\sin \theta_0)^5 \cos \theta_0 (\sin \theta_1)^3 \cos \theta_1 (\sin \theta_2)^5 \cos \theta_2 d\theta_0 d\theta_1 d\theta_2 d\chi_0 d\chi_1 d\chi_2 d\chi_3.$$

Since our analysis removes all single-photon deformation, we can leverage the fact that the only state affected by the interaction is $|1_\xi\rangle_a \otimes |1_\xi\rangle_b$ and that our gate conserves photon number to write

$$F_1(\phi) = \frac{1}{10} (6 + 3\text{Re}(e^{i\phi}\mathcal{F}) + |\mathcal{F}|^2). \quad (\text{A2})$$

Here \mathcal{F} is the overlap between the single- and two-photon wave packets:

$$\mathcal{F} = \int [\xi_1^{\text{out}}(\nu_a, \nu_b)]^* \xi_2^{\text{out}}(\nu_a, \nu_b) d\nu_a d\nu_b, \quad (\text{A3})$$

where

$$\xi_i^{\text{out}}(\nu_a, \nu_b) = \int \xi_i^{\text{in}}(\omega_a) \xi_i^{\text{in}}(\omega_b) \langle \nu_a \nu_b | S_i | \omega_a \omega_b \rangle d\omega_a d\omega_b \quad (\text{A4})$$

for $i = 1, 2$ are the propagated two-photon wave packets, respectively, according to the S-matrices computed in Ref. [28].

Often, \mathcal{F} is used as the main figure of merit, since it relates the transformed two-photon wave packet to two copies of a single-photon wave packet, thus directly measuring undesired effects such as spectral entanglement. However, we believe that the average fidelity, for our purposes, is a more transparent and unambiguous figure of merit, because it determines how well one approximates a desired gate in the computational state space. Although the average gate fidelity is not the figure of merit that appears in the threshold theorem directly, these quantities can be related [33].

We should also point out that Shapiro, in Ref. [14], considers a slightly different figure of merit, where the average in Eq. (A1) is done over all *product* two-qubit states. Using that definition, the state $|\psi\rangle$ can be parameterized as

$$|\psi\rangle = (\cos \theta_0 |0\rangle + e^{i\chi_0} \sin \theta_0 |1\rangle)(\cos \theta_1 |0\rangle + e^{i\chi_1} \sin \theta_1 |1\rangle),$$

with the Haar measure given by

$$d\psi = 4(2\pi)^{-2} \sin \theta_0 \cos \theta_0 \sin \theta_1 \cos \theta_1 d\theta_0 d\theta_1 d\chi_0 d\chi_1,$$

and our Eq. (A2) would become

$$F_2(\phi) = \frac{1}{18} (11 + 5\text{Re}(e^{i\phi}\mathcal{F}) + 2|\mathcal{F}|^2). \quad (\text{A5})$$

We have found that both definitions lead to essentially the same results. This is illustrated in Fig. 5, where we see that $F_1 < F_2$ because F_2 is less conservative. As \mathcal{F} approaches -1 (which would correspond to a perfect CPHASE gate) the difference between $F_1(\pi)$ and $F_2(\pi)$ becomes negligible. We use Eq. (A2) because of its connections to the threshold theorem, and because it can capture other undesired effects such as e.g. entanglement breaking.

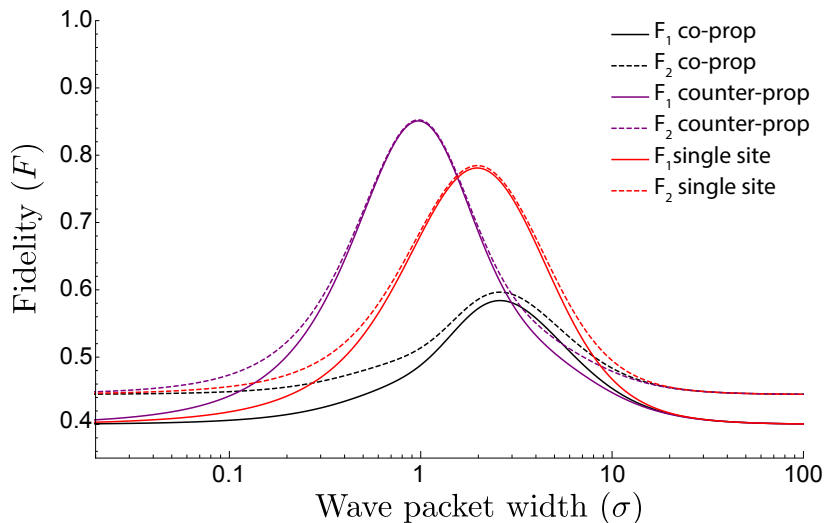


FIG. 5. (Color online). Comparison between average fidelities using a Haar average over full two-qubit Hilbert space (F_1) and over the two single-qubit Hilbert spaces (F_2). Here $\chi = 5$, $\gamma = 4.5$, and $\omega_0 = 1.1$.

Appendix B: S-matrices

For completeness, in this Appendix we write the S-matrices computed in Ref. [28]. We begin by defining the shorthands

$$\Gamma(\omega) := \frac{\gamma}{2} + i(\Delta - \omega),$$

$$\Gamma_i(\omega) := \frac{\gamma_i}{2} + i(\Delta_i - \omega_i),$$

which will be used when we have a single and multiple sites, respectively. Although we computed some of these S-matrices with different parameters ($\gamma_i, \Delta_i, \chi_i$) for each site, in the numerical work reported in the main text we assume them to be equal at all sites for simplicity.

a. Single site

For a single interaction site, the S-matrices for co- and counter-propagating photons are equivalent. In this case, we have the single-photon S-matrix

$$S_{\text{act},1}(\omega_k; \nu_k) = -\frac{\Gamma^*(\omega_k)}{\Gamma(\omega_k)} \delta(\omega_k - \nu_k).$$

for $k = a, b$. The two-photon S-matrix is

$$S_{\text{act},2}(\omega_a, \omega_b; \nu_a, \nu_b) = S_{\text{act},1}(\omega_a; \nu_a) S_{\text{act},1}(\omega_b; \nu_b) - i \frac{\chi \gamma^2}{\pi} \left(1 + \frac{2i\chi}{\Gamma(\omega_a) + \Gamma(\omega_b)} \right)^{-1} \frac{\delta(\omega_a + \omega_b - \nu_a - \nu_b)}{\Gamma(\nu_b) \Gamma(\nu_a) \Gamma(\omega_b) \Gamma(\omega_a)},$$

b. Two sites, co-propagating photons

For two interaction sites in the co-propagating arrangement, we have the single-photon S-matrix

$$S_{\text{act},1}(\omega_k; \nu_k) = \frac{\Gamma_2^*(\omega_k) \Gamma_1^*(\omega_k)}{\Gamma_2(\omega_k) \Gamma_1(\omega_k)} \delta(\omega_k - \nu_k)$$

for $k = a, b$. The two-photon S-matrix is

$$\begin{aligned}
S_{\text{act},2}(\omega_a, \omega_b; \nu_a, \nu_b) &= S_{\text{act},1}(\omega_a; \nu_a) S_{\text{act},1}(\omega_b; \nu_b) - \frac{\delta(\omega_a + \omega_b - \nu_a - \nu_b)}{\pi} \\
&\times \left[i \left(\frac{\Gamma_2^*(\omega_a) \Gamma_2^*(\omega_b)}{\Gamma_2(\omega_a) \Gamma_2(\omega_b)} \right) \left(1 + \frac{2i\chi_1}{\Gamma_1(\omega_a) + \Gamma_1(\omega_b)} \right)^{-1} \frac{\chi_1 \gamma_1^2}{\Gamma_1(\nu_b) \Gamma_1(\nu_a) \Gamma_1(\omega_b) \Gamma_1(\omega_a)} \right. \\
&+ i \left(\frac{\Gamma_1^*(\omega_a) \Gamma_1^*(\omega_b)}{\Gamma_1(\omega_a) \Gamma_1(\omega_b)} \right) \left(1 + \frac{2i\chi_2}{\Gamma_2(\omega_a) + \Gamma_2(\omega_b)} \right)^{-1} \frac{\chi_2 \gamma_2^2}{\Gamma_2(\nu_b) \Gamma_2(\nu_a) \Gamma_2(\omega_b) \Gamma_2(\omega_a)} \\
&+ \left(1 + \frac{2i\chi_1}{\Gamma_1(\omega_a) + \Gamma_1(\omega_b)} \right)^{-1} \left(1 + \frac{2i\chi_2}{\Gamma_2(\omega_a) + \Gamma_2(\omega_b)} \right)^{-1} \frac{4\chi_1 \chi_2 \gamma_1^2 \gamma_2^2}{\Gamma_1(\nu_b) \Gamma_1(\nu_a) \Gamma_2(\omega_b) \Gamma_2(\omega_a)} \\
&\left. \times \frac{1}{(\Gamma_1(\omega_a) + \Gamma_1(\omega_b))(\Gamma_1(\omega_a) + \Gamma_2(\omega_b))(\Gamma_2(\omega_a) + \Gamma_2(\omega_b))} \right].
\end{aligned}$$

c. Two sites, counter-propagating photons

For two interaction sites in the counter-propagating arrangement, the single-photon S-matrix is obviously the same as for the co-propagating arrangement. The two-photon S-matrix, however, is

$$\begin{aligned}
S_{\text{act},2}(\omega_a, \omega_b; \nu_a, \nu_b) &= S_{\text{act},1}(\omega_a; \nu_a) S_{\text{act},1}(\omega_b; \nu_b) - \frac{\delta(\omega_a + \omega_b - \nu_a - \nu_b)}{\pi} \\
&\times \left[i \left(\frac{\Gamma_2^*(\omega_a) \Gamma_2^*(\nu_b)}{\Gamma_2(\omega_a) \Gamma_2(\nu_b)} \right) \left(1 + \frac{2i\chi_1}{\Gamma_1(\omega_a) + \Gamma_1(\omega_b)} \right)^{-1} \frac{\chi_1 \gamma_1^2}{\Gamma_1(\nu_b) \Gamma_1(\nu_a) \Gamma_1(\omega_b) \Gamma_1(\omega_a)} \right. \\
&+ i \left(\frac{\Gamma_1^*(\nu_a) \Gamma_1^*(\omega_b)}{\Gamma_1(\nu_a) \Gamma_1(\omega_b)} \right) \left(1 + \frac{2i\chi_2}{\Gamma_2(\omega_a) + \Gamma_2(\omega_b)} \right)^{-1} \frac{\chi_2 \gamma_2^2}{\Gamma_2(\nu_b) \Gamma_2(\nu_a) \Gamma_2(\omega_b) \Gamma_2(\omega_a)} \left. \right].
\end{aligned}$$

d. N sites, counter-propagating photons

For the N -site case, we only computed the S-matrices in the counter-propagating arrangement, and under the assumption of translation invariance, i.e. $\gamma_i = \gamma$, $\Delta_i = \Delta$, and $\chi_i = \chi$. From this, we obtain the single-photon S-matrix

$$S_{\text{act},1}(\omega_k; \nu_k) = \left(-\frac{\Gamma^*(\omega_k)}{\Gamma(\omega_k)} \right)^N \delta(\omega_k - \nu_k),$$

for $k = a, b$, and the two-photon S-matrix is

$$\begin{aligned}
S_{\text{act},2}(\omega_a, \omega_b; \nu_a, \nu_b) &= S_{\text{act},1}(\omega_a; \nu_a) S_{\text{act},1}(\omega_b; \nu_b) - i \frac{\chi \gamma^2}{\pi} \left(1 + \frac{2i\chi}{\Gamma(\nu_b) + \Gamma(\nu_a)} \right)^{-1} \frac{\delta(\omega_a + \omega_b - \nu_a - \nu_b)}{\Gamma(\nu_b) \Gamma(\nu_a) \Gamma(\omega_b) \Gamma(\omega_a)} \\
&\times \left[\sum_{j=1}^N \left(\frac{\Gamma^*(\omega_a) \Gamma^*(\nu_b)}{\Gamma(\omega_a) \Gamma(\nu_b)} \right)^{N-j} \left(\frac{\Gamma^*(\omega_b) \Gamma^*(\nu_a)}{\Gamma(\omega_b) \Gamma(\nu_a)} \right)^{j-1} \right].
\end{aligned}$$

Appendix C: Problem statement and rules for passive CPHASE gate via cross-Kerr interactions

In this section we update Gea-Banacloche's [15] suggested requirements for proposals of CPHASE gates. Paraphrasing, Gea-Banacloche's [15] requirements were: (GB1) clearly local and physically realizable Hamiltonians; (GB2) localized wave packets using quantized multimode fields; (GB3) report gate fidelities computed; and (GB4) a realistic estimate of any residual losses or decoherence mechanisms.

We are particularly interested in determining if it is possible to construct a passive CPHASE gate using cross-Kerr interactions with the photons entering the device synchronously. By passive, we mean there should be no control pulses applied to the medium (atoms) unless they are static, and no active error correction.

We suggest the following requirements for "in principle" theory proposals

P1: Microscopic model.

Ideally, the medium should be constructed from a microscopic model using clearly local, passive, and physically realizable Hamiltonians. If the model is a hybrid model, e.g. light coupling to a spin wave, one must actually model the coupling efficiency of this interface. This is comparable to (GB1).

One point which is often overlooked is that results obtained using particular phenomenological models cannot be extended as “physical principles”, since a different medium could be constructed, out of different microscopic components, for which that result does not apply.

P2: Multimode analysis.

The analysis should be done with a quantized multimode single photons, e.g. $|1_\xi\rangle = \int d\nu \xi(\nu) a^\dagger(\nu) |0\rangle$ where $[a(\omega), a^\dagger(\nu)] = \delta(\omega - \nu)$. If possible report the relevant S-matrices or the output wave functions. This is an extension to (GB2).

P3: Reflection must be explicitly dealt with.

Either the proposal should use circulators or isolators to remove reflection altogether, or it should be shown theoretically that reflection can be suppressed enough to obtain a high-fidelity operation. For example, in proposals using continuous mediums, like atomic vapours, reflection is not usually modelled.

P4: Quality of the operation.

Standard figures-of-merit are the average gate fidelity and the diamond norm between the proposal and the CPHASE gate, restricted to the encoded state space. This is comparable to (GB3).

P5: Imperfections.

After making a convincing case for a particular theory proposal, one should then take imperfections into account. Examples include loss out of guided modes and coupling atoms (Kerr medium) to a thermal reservoir. However, it is important to keep in mind that the final word in the feasibility of any proposal is that of experiments. This means that the final proposal should model all (and only) realistic sources of noise for a particular implementation, and that results derived from this procedure should not be generalized to other experimental implementations. Finally, at this point it might be worthwhile to determine the fault tolerance threshold for the proposed imperfect gate. These points are made in (GB4).

We now also point out a few things that, in our view, might **not** be necessary.

P6: Perfect operation.

It is not necessary that the operation is perfect, or that it can be made arbitrarily good. The threshold theorem of fault-tolerant quantum computing guarantees that there exist some **constant** threshold above which error correction can be used to perform arbitrarily-long computations (this is why the average gate fidelity or the diamond norm should be used, see point P4 above). The exact value of the threshold is dependent on the noise model which should include, among other effects, the imperfections from point P5 above.

P7: Single-photon distortion.

It is preferable to obtain a high-fidelity operation without deformation of single-photon wave packets. But, as we argued in the main text, that might not be strictly necessary since there are a number of ways to work around it.